

1 Curcumin combined with Glu-GNPs enhancing radiosensitivity of transplanted tumor
2 of MDA-MB-231-luc cells in nude mice

3 Short title: Curcumin enhanced radiosensitivity

4 Mengjie Li[¶], Tingting Guo[¶], Yujian Wu, Jiayi Lin, Ke Yang, Chenxia Hu*

5

6

7

8 School of Pharmaceutical Science, Guangzhou University of Chinese Medicine, Guangzhou,

9 Guangdong, China

10

11 * Corresponding authors: Chenxia Hu*

12 Email: Huchenxia12@163.com (CXH)

13

14

15 [¶] This authors contributed equally to this work.

16

17

18

19

20

21

22

23

24

25

26

27

28

29

30

31

32

33

34

35

36 **Abstract**

37 Breast cancer is the first cause of cancer death in women all over the world. And
38 the morbidity of breast cancer has been increasing in recent years. Nowadays, the
39 treatment of breast cancer is still a problem. Radiotherapy resistance is one of the
40 important factors leading to poor prognosis of clinical treatment. Curcumin, a plant
41 polyphenol from *Curcuma longa*, has antitumor activity and inhibition of tumor
42 recurrence and metastasis. However, the influence of curcumin on radiosensitivity of
43 breast carcinoma xenografts, the synergistic effect and possible mechanism of
44 curcumin and Glucose-Gold nanoparticles (Glu-GNPs) in nude mice in vivo need to
45 be further explored. The model of transplanted tumor in nude mice was established
46 and sensitized by intravenous injection of curcumin and Glu-GNPs. The results
47 showed that curcumin can significantly inhibit the growth of tumor, and has no
48 obvious effect on the body weight of nude mice, and Curcumin, Glu-GNPs and X-ray
49 irradiation treatment alone or in combination could reduce the expression of *VEGF*
50 and *HSP90* mRNA and protein compared with model group in tumor tissue. The
51 inhibition of irradiation resistance may be related to inhibiting the synthesis of *VEGF*
52 and *HSP90*. This study suggested that curcumin and Glu-GNPs have the
53 radiosensitization effect in vivo, which provides an experimental basis for the clinical
54 development of green radiosensitizers.

55 Key words: Curcumin; Glu-GNPs; Radiosensitivity; Breast Cancer; nude mice

56

57

58 **Introduction:**

59 According to the data published by the International Cancer Research Institute in
60 2018, breast cancer has become the second leading cause of cancer related death and
61 the first one for women all over the world ^[1]. It is expected that the morbidity and
62 mortality will still increase significantly in the next few years ^[2]. Nowadays, the
63 treatment of breast cancer mainly includes surgery, chemotherapy and radiotherapy
64 ^[3-4]. Although great progress has been made in the early breast cancer treatment, there
65 is no effective strategies to deal with breast cancer metastasis. Establishing a nude
66 mouse model of breast cancer xenograft and studying the important related genes in
67 breast cancer growth and development, is an important breast cancer research method,
68 and plays a key role in studying the etiology, pathogenesis, effective prevention,
69 diagnosis and treatment, drug screening and rehabilitation of breast cancer ^[5]. In
70 recent years, bioluminescence imaging system has become a sensitive research
71 method in animal model. It can monitor the growth and metastasis of tumor in real
72 time. In addition, it can be accurately detected in vivo without killing mice ^[6]. Zhang
73 et al ^[7] found that the results of in vivo imaging and pathological detection are
74 consistent, but compared with HE staining, the growth and metastasis of breast cancer
75 can be more directly and clearly observed using in vivo imaging system. In vivo
76 imaging method is applied to study transplanted tumor in mice. Compared with
77 traditional measurement method, in vivo imaging shows scientific methods to
78 measure tumor growth more accurately, which greatly reduces the error of artificial
79 measurement.

80 The development of Gold nanoparticles (GNPs) can be traced back to the 16th
81 century. GNPs, a type of nanomaterial approved for clinical trials by FDA in the US,
82 had become a hot area in scientific research [8]. It was reported that when GNPs
83 received X-ray irradiation, the ionizing ability of the radiation to tumor cells was
84 enhanced, which promoted tumor cell damage and apoptosis [9-12]. Our previous study
85 suggested that Glu-GNPs assimilated in MCF-7 adherent cells and THP-1 suspension
86 cells were easier than GNPs and enhanced the cancer killing of THP-1 cells 20%
87 more than GNPs [13]. It pointed that glucose tagging may be a correct way to
88 promoting the uptake of GNPs in tumor cells, as tumor cells can take up more glucose
89 than normal cells. In addition, it was previously demonstrated that these nanometal
90 particles enhanced killing effects on tumor cells without increasing damage to the
91 surrounding normal tissues in a mouse model, thereby reducing the adverse effects of
92 radiotherapy [14-15].

93 In recent years, scientific research has found that traditional Chinese materia
94 medica has unique advantages and efficacy in treating tumors. Curcumin, a plant
95 polyphenol extracted from the rhizome of *Curcuma longa*, is the main ingredient of
96 curry, with the characteristics of high efficiency, safety and low toxicity [16]. It was
97 reported that curcumin has killing and therapeutic effects on many kinds of cancer
98 including lung cancer [17], gastric cancer [18] and breast cancer [19] in vitro and in vivo.
99 Hu Shan, et al [20] found that curcumin can inhibit the proliferation of various breast
100 cancer cells such as MDA-MB-231, MCF-7, MDA-MB-468 and T47D, which also
101 induced cell apoptosis. Palange's study showed that curcumin treatment can limit the

102 metastatic potential of breast cancer cell lines, possibly by altering the expression of
103 related adhesion molecules ^[21]. These findings suggested that curcumin may have
104 important research significance in the treatment of breast cancer. However, it reminds
105 to be studied whether curcumin enhances radiosensitivity effect and curcumin has
106 synergistic effect with Glu-GNPs. And the mechanism of curcumin on breast cancer
107 is not clear.

108 In this study, we used the cell line MDA-MB-231-luc to establish subcutaneous
109 transplant tumor model. The tumor-bearing mice were treated with curcumin,
110 Glu-GNPs and irradiation alone or in combination for 3 weeks. The tumor volume
111 and body weight of tumor-bearing mice were measured regularly. Tumor growth was
112 monitored by in-vivo imaging system. Our results showed that curcumin may inhibit
113 tumor growth in nude mice and reduce tumor fluorescence intensity but has no
114 obvious effect to the body weight. Further study suggested that curcumin and
115 Glu-GNPs along with X-ray irradiation can down-regulated the mRNA and protein
116 expression of *VEGF* and *HSP90*. These data showed that curcumin may be a potential
117 drug for breast cancer treatment.

118 **Materials and methods**

119 **Reagents and antibodies**

120 Curcumin(Sigma-Aldrich, Merck KGaA Darmstadt, Germany; Purity \geq 80%)was
121 dissolved in corn oil with 2% dimethyl sulfoxide(DMSO).The concentration of
122 Glu-GNPs (Beijing Dk Nanotechnology Co, Ltd, Beijing, China) is 1 mg/mL. The

123 primary antibodies [β -actin (#4970), HSP90 (#4877)] were obtained from Cell
124 Signaling Technology, VEGF (ab52917) from Abcam and the secondary antibodies
125 goat anti-rabbit and goat anti-mouse were obtained from Boster (Boster
126 Bioengineering Co, Ltd, Wuhan).

127 **Cell culture**

128 Human breast cancer cell line MDA-MB-231 cells labeled with firefly luciferase
129 (MDA-MB-231-luc) was obtained from Shanghai Soft Top Biological Company and
130 cultured in Modified Eagle's Medium (MEM) supplemented with 10% Fetal Bovine
131 Serum(FBS),100U/ml penicillin and 100 μ g/ml streptomycin(all from Gibco, USA)
132 at 37°C in a humidified incubator with an atmosphere of 5% CO₂ (Thermo fisher
133 scientific). The cells were passaged at a density of 2.0 \times 10⁵ cells in a 25cm² flask or
134 cryopreserved at a density of 2.0 \times 10⁶/mL.

135 **Detection of MDA-MB-231-luc fluorescence intensity**

136 The fluorescence intensity of MDA-MB-231-luc was measured by in-vivo
137 imaging system. Different number of cells(1.25 \times 10⁴, 2.5 \times 10⁴, 5 \times 10⁴ and 1 \times 10⁵
138 respectively)were inoculated into the black opaque 96-well plate for 4 hours to make
139 the cells attach to the well. According to the operation of the Firefly-Luciferase assay
140 kit, the cells were lysed with lysate and then added with luciferase substrate. Their
141 luminescence was detected in-vivo imaging system immediately.

142 **Establishment of subcutaneous transplanted tumors in nude** 143 **mice**

144 Female *BALB/c-nu/nu* mice aged 4-6 weeks were purchased from Guangzhou
145 University of Chinese Medicine and the scientific research was passed the animal
146 ethics examination. The nude mice were raised adaptively for 7 days and after that
147 they were randomly divided into groups including control group, model
148 group(Model), cisplatin group(Cis), curcumin group(Cur), irradiation group(IR),
149 curcumin combined with Glu-GNPs group (Cur+Glu-GNPs) and curcumin combined
150 Glu-GNPs along with irradiation group (Cur+Glu-GNPs+IR) (5-8 mice per group).
151 All nude mice except the control group were inoculated 0.1mL cell suspension
152 containing 1.5×10^7 MDA-MB-231-luc cells in phosphate-buffer saline (PBS) and
153 Matrigel (1:1) into the second pair of subcutaneous mammary glands on the left. Nude
154 mice in control group were inoculated with 0.1mL suspension of PBS and Matrigel
155 (1:1). After 3-7 days, tumors formed in the inoculated site of nude mice except the
156 control group. When the diameter of transplanted tumor was greater than 5 mm, the
157 model was successfully established. The tumor volume was measured every 3 days
158 and the body weight of mice was done every week.

159 **Tumor-bearing mice treated with drugs and irradiation**

160 The calculation method of tumor volume is as follows: $V = ab^2/2$ (a, length; b,
161 short diameter). When the volume of the tumor reached 100-200 mm³, the
162 tumor-bearing mice of Cur group were treated with curcumin (100 mg/kg curcumin

163 dissolved in corn oil contained 2% DMSO), Model group (corn oil contained 2%
164 DMSO), IR group (corn oil contained 2% DMSO), and Cur+IR group (100 mg/kg
165 curcumin dissolved in corn oil contained 2% DMSO) by intraperitoneal injection
166 every other day, and Glu-GNPs+IR group (4 mg/kg Glu-GNPs suspension) by caudal
167 vein injection weekly, and Cisplatin group (3 mg/kg cisplatin dissolved in normal
168 saline)by intraperitoneal injection every three days, or Cur+Glu-GNPs+IR (100
169 mg/kg curcumin by intraperitoneal injection every other day and 4 mg/kg Glu-GNPs
170 by caudal vein injection weekly). The treatment lasted for 3 weeks. After that, the
171 tumor-bearing mice in IR, Glu-GNPs+IR and Cur+Glu-GNPs+IR group were treated
172 with X-ray irradiation (10 Gy) by X-Ray Irradiation Cabinet (MultiRad 225, Faxitron
173 Bioptics, LLC. America). All tumor tissue was extracted from tumor-bearing mice
174 and weighted on the 24th of treatment. One part of the tumor tissue was fixed by
175 soaking in 4% polyformaldehyde solution at 4°C for HE staining and
176 immunohistochemistry assay. The other part of the tumor was transferred into liquid
177 nitrogen and stored in the refrigerator at -80°C for qRT-PCR detection.

178 **Tumor growth was monitored using in-vivo imaging system**

179 After treatment for 24 days, the tumor-bearing mice were injected 150mg/kg
180 luciferase substrate (sciencelight, shanghai, China) intraperitoneally in advance.
181 Mice were anesthetized by inhaling isoflurane during observation. The mice were
182 lying on their sides, and the tumor was exposed. The fluorescence intensity in all

183 groups of mice was detected and recorded 10 minutes after the injection by using
184 in-vivo bioluminescence imaging system.

185 **HE staining**

186 Tumor tissue samples were fixed in 4% paraformaldehyde at 4°C for 48 hours.
187 After that, the samples were dehydrated, embedded, paraffin sectioned and stained
188 according to the general process. The malignant degree of tumor cells in each group
189 was observed under microscope after sealed with neutral gum.

190 **Immunohistochemical analysis**

191 *VEGF* (*VEGF* Rabbit mAb, 1:50) and *HSP90* (*HSP90* Rabbit mAb, 1:50)
192 expression were detected by immunohistochemistry. Tumor tissue samples fixed in
193 4% polyformaldehyde solution were sliced with the paraffin-sectioning machine,
194 stained with an immunohistochemistry kit (Bioss, China), and then sealed with neutral
195 gum after dehydration of gradient ethanol solution and transparent treatment of
196 xylene. Positive cells were randomly selected five areas and counted under 400×
197 optical microscopy.

198 **Quantitative Real-Time Polymease Chain** 199 **Reaction(qRT-PCR)**

200 Total RNA was extracted using trizol (Takara, Japanese) and cDNA synthesis
201 using Takara RNA Purification Kit according to the manufacturer's instructions. The
202 amplification procedure was as follows: the first step is 95 ° C for 3 minutes, the

203 second step is at 95 ° C for 5 seconds, and 60 ° C for 30 seconds for 40 cycles, and the
204 last step ends with the Melt Curve procedure. The relative expression was evaluated
205 following the relative quantification equation, $2^{-\Delta\Delta CT}$. qPCR was performed by using
206 the following primers:

207 *ACTB*:forward:5'*GTGGCCGAGGATTTGATTG3'*;

208 reverse:5'*CCTGTAACAACGCATCTCATATT3'*

209 *GAPDH*:forward:5'*AGCCACATCGCTCAGACAC3'*;

210 reverse:5'*GCCCAATACGACCAAATCC3'*

211 *VEGF*:forward:5'*TAGAGTACATCTTCAAGCCGTC3'*;

212 reverse:5'*CTTTCTTTGGTCTGCATTACACA3'*

213 *HSP90*:forward:5'*ACGAAGCATAACGACGATGAGCAG3'*;

214 reverse:5'*CCATTGGTTCACCTGTGTCAGTCC3'*

215 **Statistical Analysis**

216 The data of multiple groups were analyzed by one-way ANOVA, and
217 subsequent analysis was performed with Student's t-tests in SPSS 19.0. Results are
218 expressed as means \pm SD. P<0.05 indicates significance.

219 **Results**

220 **Cells expressed fluorescence stably**

221 Fluorescence was observed obviously in the cells in each well by in-vivo
222 imaging system, and as the number of cells increased, the fluorescence intensity

223 increased correspondingly (Fig 1A and B). It indicated that MDA-MB-231-luc cells
224 could express luciferase stably.

225 **Fig 1. Cell culture and model establishment.** (A) The image of MDA-MB-231-luc
226 cell. (B) The fluorescence intensity of different number of cells(1.25×10^4 , 2.5×10^4 ,
227 5×10^4 and 1×10^5 respectively)were detected in-vivo imaging system in the black
228 opaque 96-well plate. (C) Breast tumor-bearing nude mice model with stable
229 luciferase expression were successfully established 3-7 days after inoculation. (D)
230 Schematic diagram of xenograft in nude mice. MDA-MB-231-luc cells were
231 transplanted into the second pair of subcutaneous mammary glands on the left. When
232 the volume of the tumor reached 100-200 mm³, curcumin in corn oil (2% DMSO),
233 Glu-GNPs, and cisplatin in saline solution were administrated regularly. After 3
234 weeks of treatment, the tumor-bearing mice (IR, Glu-GNPs+IR, Cur+IR and
235 Cur+Glu-GNPs+IR groups) were treated with irradiation (10Gy). Three days later,
236 nude mice of each group were detected fluorescence intensity by in-vivo imaging
237 system.

238 **Transplanted tumors in nude mice model was established**
239 **successfully**

240 Three to seven days after inoculated, nude mice formed tumors gradually and the
241 tumor formation rate was 100% except for control group (Fig 1C). The shape of the
242 tumor was close to sphere, and a few of them were irregular. Meanwhile, there was no
243 significant change in body weight of tumor-bearing mice. When the volume of the

244 tumor reached 100-200 mm³, the tumor-bearing mice were treated with different
245 drugs for 3 weeks regularly (Fig 1D).

246 **Tumor growth was inhibited by curcumin**

247 During treatment, the tumor volume was measured every 3 days and the body
248 weight of tumor-bearing mice were measured every other week. Cisplatin was used as
249 positive control. Change of tumor volume suggested that tumor volume in model
250 group increased rapidly, while tumor growth in other treated groups was slower than
251 that in model group, of which the cisplatin group grew slowly relatively and the tumor
252 volume decreased less ($p < 0.001$). After irradiation treatment, the tumor volume of
253 mice irradiated by X-ray decreased significantly, especially in Cur+Glu-GNPs+IR
254 group (Fig 2A). Before radiotherapy treatment, the body weight of mice did not
255 decrease obviously except for cisplatin group. After 3 weeks of medication, the
256 tumor-bearing mice containing the irradiation group received X-ray treatment. After
257 irradiation, the body weight of the mice decreased significantly and
258 mice were generally in poor condition. Meanwhile, the body weight loss of mice in
259 cisplatin group was still going on and two of them died, while there was no dead mice
260 in curcumin group (Fig 2B). These results showed that curcumin can inhibit tumor
261 growth without obvious toxic and side effects. The body weight of mice in
262 Cur+Glu-GNPs+IR group decreased significantly, indicating that X-ray irradiation
263 had a bad impact on the survival of mice. After sampled, the tumor tissue was
264 weighed, and the tumor weight of each administration group was statistically different

265 from that of the model group (Fig 2C and D). The tumor weight of cisplatin group,
266 Cur+IR group and Cur+Glu-GNPs+IR group were reduced compared with model
267 group. The results showed that curcumin combined Glu-GNPs along with radiation
268 played a synergistic therapeutic effect on breast cancer tumor growth.

269 **Fig 2. Tumor growth decreased after the treatment of curcumin, Glu-GNPs and**
270 **radiation, alone and in combination.** (A) Tumor volumes were measured every four
271 days. The data was normalized to the model. P values were determined by the Student
272 's t test. *P<0.05 and **P<0.01 vs. Model group; (B) The weight of nude mice was
273 measured weekly. (C) Images of transplanted tumor tissues. The tumor tissues were
274 removed after treatment. (D) Tumor tissues weight was detected. The data was
275 normalized to the Model group. Error bars indicate SD. *P<0.05, **P<0.01 and ***P<0.01 vs.
276 Model group (Student 's t test).

277 **Changes of fluorescence intensity in-vivo imaging system**

278 The fluorescence intensity of tumor growth was monitored 24 days after
279 treatment, by in-vivo imaging system. We randomly selected two tumor-bearing
280 mice in each group to detect their fluorescence intensity. The results showed that the
281 fluorescence intensity of the model group was the highest among all tumor-bearing
282 mice. Compared with the model group, the fluorescence intensity in cisplatin group
283 and Cur+Glu-GNPs+IR group decreased significantly (Fig 3). It also showed that
284 curcumin can inhibit tumor fluorescence intensity. And there was synergistic effect
285 in curcumin combined Glu-GNPs along with radiation.

286 Fig 3. **Changes of fluorescence intensity in-vivo imaging.** After treatment, the
287 fluorescence intensity of tumor-bearing mice injected luciferase substrate (150mg/kg)
288 intraperitoneally in advance was monitored by in-vivo bioluminescence imaging
289 system, and represented by the color. Mice were anesthetized by inhaling isoflurane.
290 The fluorescence was observed under the same condition.

291 **Morphological changes of tumor tissues after treatment**

292 After HE staining, the morphology of tumor tissue sections (4 μ m) in each group
293 were observed under microscope. The nucleus of tumor cells was large and
294 heterogeneity, almost no cytoplasm, with more necrosis in the center of the tumor.
295 The results showed that breast carcinoma xenograft was invasive ductal carcinoma
296 with high malignancy. (Fig 4A).

297 Fig 4. **Detection of tumor tissue samples.** (A) Representative images of HE
298 staining(400 \times). HE staining depicts malignant degree of xenograft and form of tumor
299 cells. The cells of tumor tissues had large and dark nuclei, almost no cytoplasm, with
300 more necrosis in the center of the tumor. Arrows point to tumor cells. qRT-PCR
301 analyses of the mRNA levels of *HSP90*(B) and *VEGF*(C) in tumor tissue.
302 *β -actin* was used as reference gene. The data was analyzed with the mean \pm SD of
303 three times of independent experiments. * $P < 0.05$ vs. Model group (Student 's t test).
304 (D) Representative images of IHC staining(400 \times) of *HSP90* and *VEGF*. Tumor tissue
305 was immunostained using DAB (brown) and Haematoxylin (blue) for nuclear

306 counterstaining. Arrows point to nuclear expression of *HSP90* or *VEGF* in breast
307 cancer cells respectively. Scale bars, 20 μ m.

308 **mRNA level is regulated after treatment**

309 The mRNA level of *VEGF* and *HSP90* was examined by qRT-PCR. Compared
310 with model group, The mRNA level of *VEGF* [(Cisplatin (~0.42-fold), Cur
311 (~0.87-fold), IR (~0.87-fold), Cur+IR (~0.55-fold), Glu-GNPs+IR (~0.61-fold), and
312 Cur+Glu-GNPs+IR(~0.46-fold)] and
313 *HSP90*[(Cisplatin(~0.54-fold),Cur(~1.28-fold),IR(~0.74-fold),Cur+IR(~0.92-fold),Gl
314 u-GNPs+IR(~0.65-fold),and Cur+Glu-GNPs+IR(~0.40-fold)] were regulated(Fig. 6A
315 and B).These results showed that curcumin and radiation can both down-regulate the
316 expression level of *VEGF* in tumor tissue, especially Cur+Glu-GNPs+IR group
317 significantly ($P < 0.05$). In addition, curcumin can down-regulate the mRNA level of
318 *HSP90*. When curcumin combined Glu-GNP along with radiation, the expression
319 level of *HSP90* decreased significantly compared with model group ($P < 0.05$) (Fig
320 4B and C). It was suggested that curcumin combined Glu-GNPs along with radiation
321 may be related to the effective inhibition of *VEGF* and *HSP90* in breast tumor tissue.

322 **Immunohistochemical analysis of VEGF and HSP90 gene**

323 Five areas were randomly selected under the microscope, of which brown was
324 positive expression. The expression level of *VEGF* decreased in curcumin group,
325 especially in cisplatin group and Cur+Glu-GNPs+IR group. *HSP90* expression in

326 radiation group was higher than that in model group, but decreased after curcumin
327 treatment (Fig 4D). Radiation can promote the expression of *HSP90*, while curcumin
328 combined with irradiation can down regular the level of *HSP90*, protect normal cells
329 and inhibit the growth of tumor cells. The results showed that curcumin can inhibit
330 the growth of tumor vessels and had synergistic effect along with Glu-GNPs and
331 X-ray therapy.

332 **Discussion**

333 Curcumin is a plant polyphenol with effective activities and is also used as food
334 in daily life. Nowadays, studies have reported that curcumin has anti-cancer activity,
335 low toxicity and side effects. Our previous studies showed that curcumin has an
336 effective inhibition on MDA-MB-231 and MCF-7 cells [22]. It has been reported that
337 curcumin combined with a variety of anti-cancer drugs can enhance the sensitivity of
338 cancer cells, which has become a research direction. In addition, our previous studies
339 had demonstrated that Glu-GNPs may be a promising radiosensitizer which exerted
340 radiosensitizing effect on MDA-MB-231 adherent cells and stem cells. However, the
341 influence of curcumin on radiosensitivity of breast carcinoma in vivo and the
342 synergistic effect with Glu-GNPs are not clear.

343 In this study, we selected luciferase-labeled cell line MDA-MB-231-luc, and
344 established transplanted tumor model by subcutaneous inoculated of cells into the
345 underarm of mice, with a tumor formation rate of 100%. Then nude mice were treated
346 for 3 weeks, cisplatin was used as positive drug. According to the growth rate of

347 tumor volume and the body weight of mice, the curative effect of drugs was
348 preliminarily evaluated. We found that cisplatin was effective in the treatment
349 process, but the body weight loss of mice in cisplatin group was obvious.
350 Curcumin-containing group could not only inhibit tumor growth, but also had little
351 effect on the body weight of tumor-bearing mice.

352 After that, we observed the tumor fluorescence intensity of each group of
353 tumor-bearing mice through in-vivo imaging assay. The results showed that the tumor
354 fluorescence intensity in the model group was the highest, while in the
355 Cur(100mg/kg) group, Cur+IR group and Cur+Glu-GNPs group, the fluorescence
356 intensity is relatively weakened. The decrease was the most obvious in
357 Cur+Glu-GNPs+IR group (Tumor growth rate=5.92%) and cisplatin group (Tumor
358 growth rate=5.31%).Therefore, it can be concluded that curcumin can effectively
359 inhibit the growth rate of transplanted tumor, and combined Glu-GNPs along with
360 X-ray has synergistic therapeutic effect.

361 Studies have shown that its radiotherapy resistance mechanism is that blood
362 vessels are irregularly distributed in tumor tissue, blood circulation is blocked,
363 hypoxic areas exist in tumor tissue, hypoxic cells have high radiation tolerance and
364 DNA damage of tumor stem cells [23]. Therefore, the combination of drugs and
365 irradiation may be sensitive to tumor cells. In this study, we found that curcumin
366 combined with Glu-GNPs can significantly reduce *VEGF* mRNA and protein levels
367 ($p < 0.05$), and it can reduce HSP90 production in tumor tissue. *VEGF* is an
368 angiogenesis factor in mice and plays an important role in tumor growth. The level of

369 *VEGF* can be used as a marker to assess tumor status. *HSP90* is a kind of stress
370 protein, which can rise sharply and promote the growth of tumors when stimulated by
371 the environment. The results suggested that curcumin can inhibit the generation of
372 blood vessels and *HSP90* in breast cancer transplanted tumor, thus inhibiting the
373 growth of tumor and promoting the killing effect of radiation on tumor cells.

374 **Acknowledgments**

375 The author would like to thank the Animal Ethics Committee of Guangzhou
376 University of Chinese Medicine for its support and the experimental platform
377 provided by School of Basic Medical Science.

378 **Author Contributions**

379 Data curation: Mengjie Li, Tingting Guo, Chenxia Hu.

380 Formal analysis: Mengjie Li, Tingting Guo, Yujian Wu.

381 Investigation: Mengjie Li, Tingting Guo, Ke Yang, Chenxia Hu.

382 Methodology: Mengjie Li, Tingting Guo, Chenxia Hu.

383 Project administration: Chenxia Hu

384 Software: Yujian Wu, Ke Yang, Jiayi Lin, Mengjie Li.

385 Supervision: Chenxia Hu.

386 Writing-original draft: Mengjie Li, Yujian Wu.

387 Writing-review & editing : Mengjie Li, Jiayi Lin, Tingting Guo, Ke Yang, Chenxia
388 Hu.

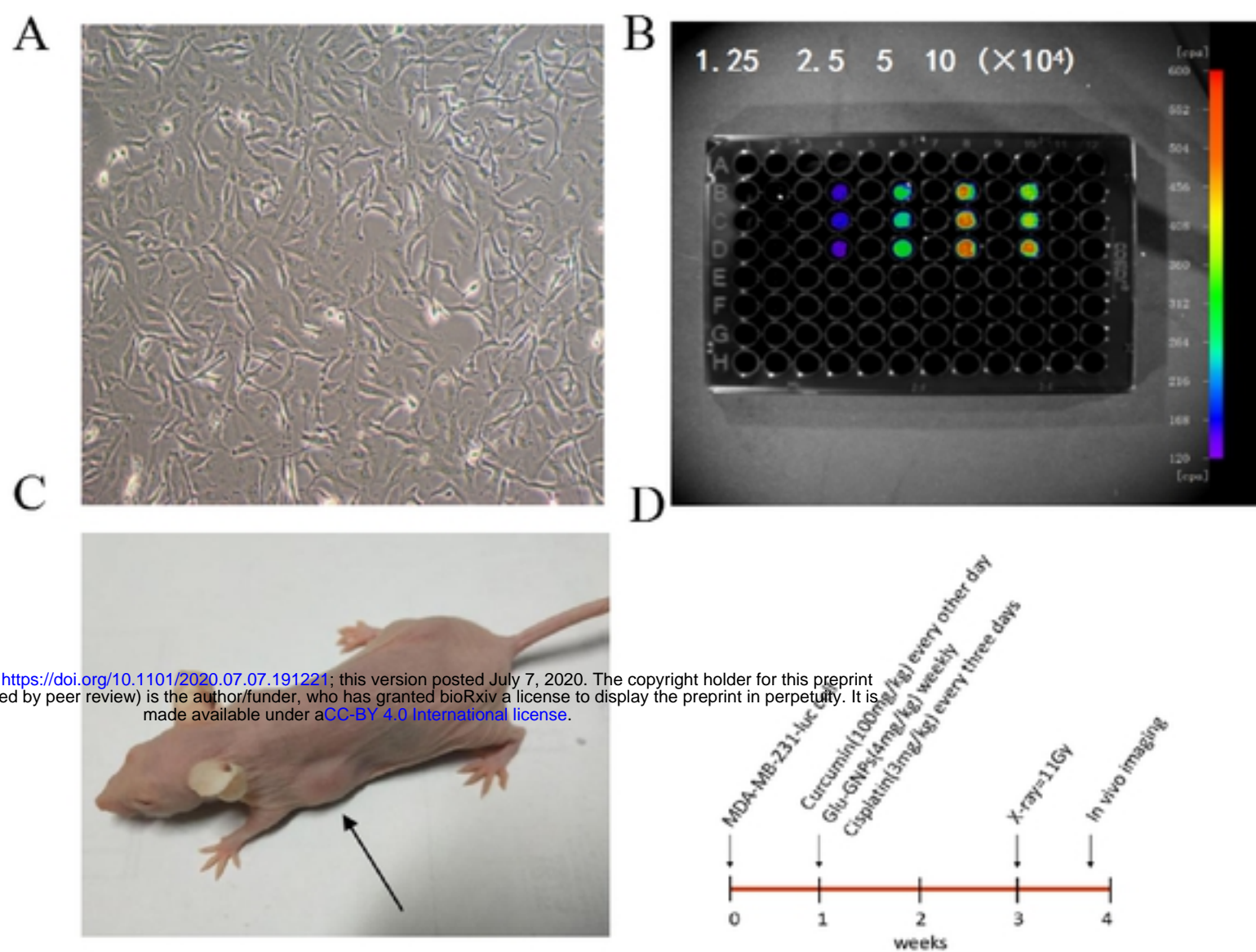
389 **References**

- 390 [1] Bray F, Ferlay J, Soerjomataram I, Siegel RL, Torre LA, Jemal A. Global cancer statistics
391 2018: GLOBOCAN estimates of incidence and mortality worldwide for 36 cancers in 185
392 countries. *CA Cancer J Clin.* 2018;68(6):394-424. <http://doi.org/10.3322/caac.21492>
393 PMID:[30207593](https://pubmed.ncbi.nlm.nih.gov/30207593/)
- 394 [2] Zhang C, Samanta D, Lu H, Bullen WJ, Zhang U, Chen I, et al. Hypoxia induces the breast
395 cancer stem cell phenotype by HIF-dependent and ALKBH5-mediated m⁶A-demethylation of
396 NANOG mRNA. *Proc Natl Acad Sci U S A.* 2016;113(14): E2047-E2056.
397 <http://doi.org/10.1073/pnas.1602883113> PMID:[27001847](https://pubmed.ncbi.nlm.nih.gov/27001847/)
- 398 [3] Anastasiadi Z, Lianos GD, Ignatiadou E, Harissis HV, Mitsis M. Breast cancer in young
399 women: an overview. *Updates Surg.* 2017; 69(3):313-317.
400 <http://doi.org/10.1007/s13304-017-0424-1> PMID:[28260108](https://pubmed.ncbi.nlm.nih.gov/28260108/)
- 401 [4] Fredholm H, Eaker S, Frisell J, Holmberg L, Fredriksson I, Lindman H. Breast cancer in
402 young women: poor survival despite intensive treatment. *PLoS One.* 2009; 4(11): e7695.
403 <http://doi.org/10.1371/journal.pone.0007695> PMID:[19907646](https://pubmed.ncbi.nlm.nih.gov/19907646/)
- 404 [5] Caglevic C, Anabalón J, Soza C, et al. Triple-negative breast cancer: the reality in Chile and in
405 Latin America. *Ecancermedicalscience.* 2019; 13:893. Published 2019 Jan 22.
406 <http://doi.org/10.3332/ecancer.2019.893> PMID:[30792810](https://pubmed.ncbi.nlm.nih.gov/30792810/)
- 407 [6] Grisez BT, Ray JJ, Bostian PA, Markel JE, Lindsey BA. Highly metastatic K7M2 cell line: A
408 novel murine model capable of in vivo imaging via luciferase vector transfection [published
409 online ahead of print, 2018 Feb 10]. *J Orthop Res.* 2018;10.1002/jor.23868.
410 <http://doi.org/10.1002/jor.23868> PMID:[29427436](https://pubmed.ncbi.nlm.nih.gov/29427436/)

- 411 [7] Zhang Y, Zhang GL, Sun X, Gao KX, Cong M, Nan N, et al. Establishment of a murine breast
412 tumor model by subcutaneous or orthotopic implantation. *Oncol Lett.* 2018;15(5):6233-6240.
413 <http://doi.org/10.3892/ol.2018.8113> PMID:[29616105](#)
- 414 [8] Kim BY, Rutka JT, Chan WC. *Nanomedicine.* *N Engl J Med.* 2010;363(25):2434-2443.
415 <http://doi.org/10.1056/NEJMra0912273> PMID:[21158659](#)
- 416 [9] Hirsch LR, Stafford RJ, Bankson JA, Sershen SR, Rivera B, Price RE, et al. Nanoshell-mediated
417 near-infrared thermal therapy of tumors under magnetic resonance guidance. *Proc Natl Acad Sci U S*
418 *A.* 2003;100(23):13549-13554. <http://doi.org/10.1073/pnas.2232479100> PMID:[14597719](#)
- 419 [10] Zhang F, Zhang T, Gu ZP, Zhou YA, Han Y, Li XF, et al. Enhancement of radiosensitivity by
420 roscovitine pretreatment in human non-small cell lung cancer A549 cells. *J Radiat Res.*
421 2008;49(5):541-548. <http://doi.org/10.1269/jrr.08024> PMID:[18728343](#)
- 422 [11] Kong T, Zeng J, Wang X, Yang XY, Yang J, McQuarrie S, et al. Enhancement of radiation
423 cytotoxicity in breast-cancer cells by localized attachment of gold nanoparticles. *Small.*
424 2008;4(9):1537-1543. <http://doi.org/10.1002/smll.200700794> PMID:[18712753](#)
- 425 [12] Roa W, Zhang X, Guo L, Shaw A, Hu XY, Xiong Y, et al. Gold nanoparticle sensitize
426 radiotherapy of prostate cancer cells by regulation of the cell cycle. *Nanotechnology.*
427 2009;20(37):375101. <http://doi.org/10.1088/0957-4484/20/37/375101> PMID:[19706948](#)
- 428 [13] Hu C, Niestroj M, Yuan D, Chang S, Chen J. Treating cancer stem cells and cancer metastasis
429 using glucose-coated gold nanoparticles. *Int J Nanomedicine.* 2015; 10:2065-2077. Published 2015
430 Mar 16. <http://doi.org/10.2147/IJN.S72144> PMID:[25844037](#)
- 431 [14] Loo C, Lowery A, Halas N, West J, Drezek R. Immunotargeted nanoshells for integrated cancer
432 imaging and therapy. *Nano Lett.* 2005;5(4):709-711. <http://doi.org/10.1021/nl050127s>

- 433 PMID:[15826113](https://pubmed.ncbi.nlm.nih.gov/15826113/)
- 434 [15] Le Goas M, Paquet M, Paquirissamy A, Guglielmi J, Compin C, Thariat J, et al.
435 Improving ¹³¹I Radioiodine Therapy by Hybrid Polymer-Grafted Gold Nanoparticles. Int J
436 Nanomedicine. 2019; 14:7933-7946. Published 2019 Sep 30. <http://doi.org/10.2147/IJN.S211496>
437 PMID:[31686819](https://pubmed.ncbi.nlm.nih.gov/31686819/)
- 438 [16] Colacino JA, McDermott SP, Sartor MA, Wicha MS, Rozek LS. Transcriptomic profiling of
439 curcumin-treated human breast stem cells identifies a role for stearyl-coa desaturase in breast
440 cancer prevention. Breast Cancer Res Treat. 2016;158(1):29-41.
441 <http://doi.org/10.1007/s10549-016-3854-4> PMID:[27306423](https://pubmed.ncbi.nlm.nih.gov/27306423/)
- 442 [17] Su W, Wei T, Lu M, Meng Z, Chen X, Jing J, et al. Treatment of metastatic lung cancer via
443 inhalation administration of curcumin composite particles based on mesoporous silica. Eur J
444 Pharm Sci. 2019; 134:246-255. <http://doi.org/10.1016/j.ejps.2019.04.025> PMID:[31032984](https://pubmed.ncbi.nlm.nih.gov/31032984/)
- 445 [18] Wang XP, Wang QX, Lin HP, Chang N. Anti-tumor bioactivities of curcumin on mice
446 loaded with gastric carcinoma. Food Funct. 2017;8(9):3319-3326.
447 <http://doi.org/10.1039/c7fo00555e> PMID:[28848967](https://pubmed.ncbi.nlm.nih.gov/28848967/)
- 448 [19] Shen Y, Han Z, Liu S, Jiao Y, Li Y, Yuan H. Curcumin Inhibits the Tumorigenesis of Breast
449 Cancer by Blocking Tafazzin/Yes-Associated Protein Axis. Cancer Manag Res. 2020;
450 12:1493-1502. <http://doi.org/10.2147/CMAR.S246691> PMID:[32161501](https://pubmed.ncbi.nlm.nih.gov/32161501/)
- 451 [20] Hu S, Xu Y, Meng L, Huang L, Sun H. Curcumin inhibits proliferation and promotes
452 apoptosis of breast cancer cells. Exp Ther Med. 2018;16(2):1266-1272.
453 <http://doi.org/10.3892/etm.2018.6345> PMID:[30116377](https://pubmed.ncbi.nlm.nih.gov/30116377/)

- 454 [21] Palange AL, Di Mascolo D, Singh J, Franceschi MSD, Carullo C, Gnasso A, et al.
455 Modulating the vascular behavior of metastatic breast cancer cells by curcumin treatment. *Front*
456 *Oncol.* 2012; 2:161. Published 2012 Nov 15. <http://doi.org/10.3389/fonc.2012.00161>
457 PMID:[23162792](https://pubmed.ncbi.nlm.nih.gov/23162792/)
- 458 [22] Hu C, Li M, Guo T, Wang S, Huang W, Yang K, et al. Anti-metastasis activity of curcumin
459 against breast cancer via the inhibition of stem cell-like properties and EMT. *Phytomedicine.*
460 2019; 58:152740. <http://doi.org/10.1016/j.phymed.2018.11.001> PMID:[31005718](https://pubmed.ncbi.nlm.nih.gov/31005718/)
- 461 [23] Barker HE, Paget JT, Khan AA, Harrington KJ. The tumour microenvironment after
462 radiotherapy: mechanisms of resistance and recurrence. *Nat Rev Cancer.* 2015;15(7):409-425.
463 <http://doi.org/10.1038/nrc3958> PMID:[26105538](https://pubmed.ncbi.nlm.nih.gov/26105538/)



bioRxiv preprint doi: <https://doi.org/10.1101/2020.07.07.191221>; this version posted July 7, 2020. The copyright holder for this preprint (which was not certified by peer review) is the author/funder, who has granted bioRxiv a license to display the preprint in perpetuity. It is made available under aCC-BY 4.0 International license.

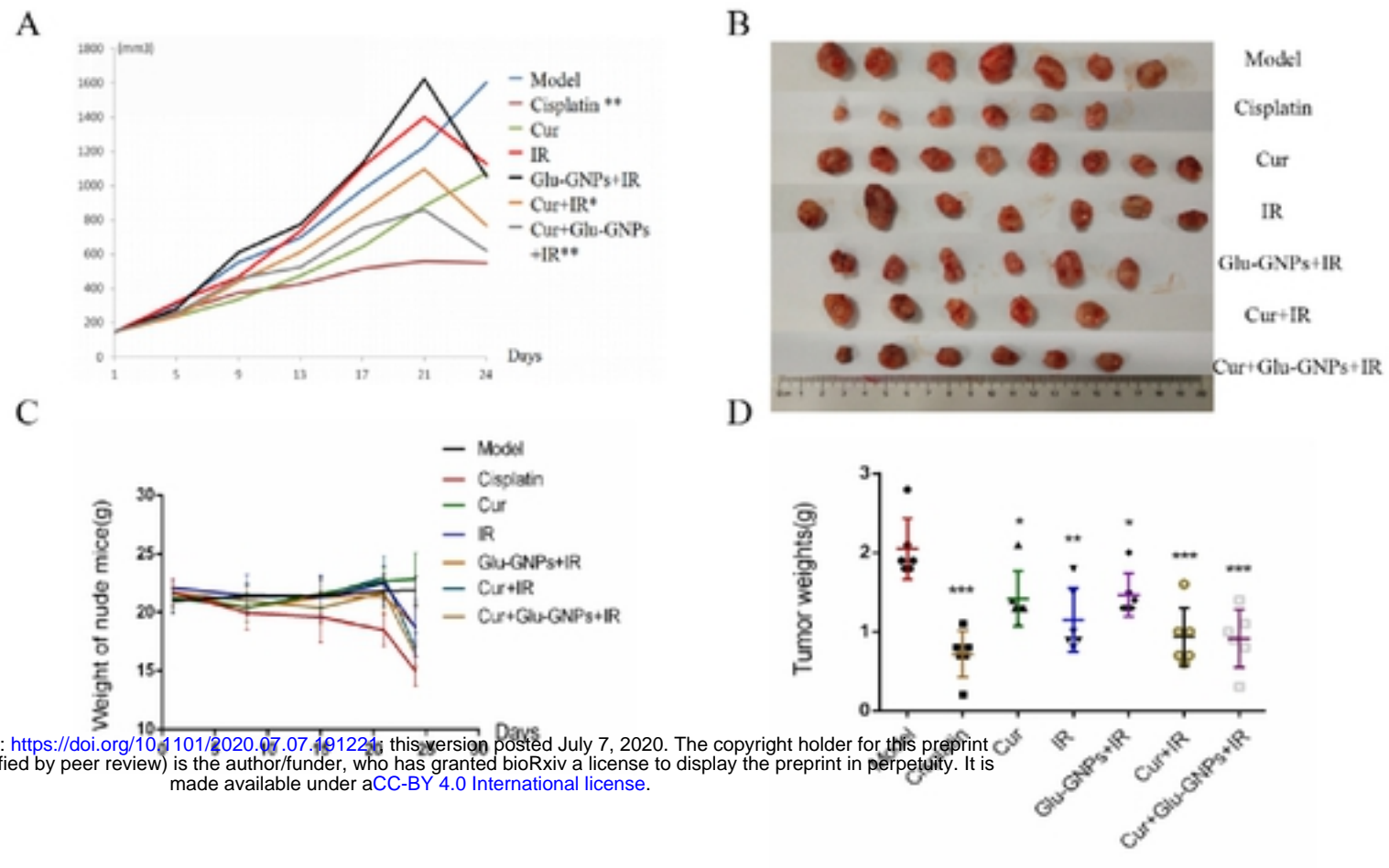
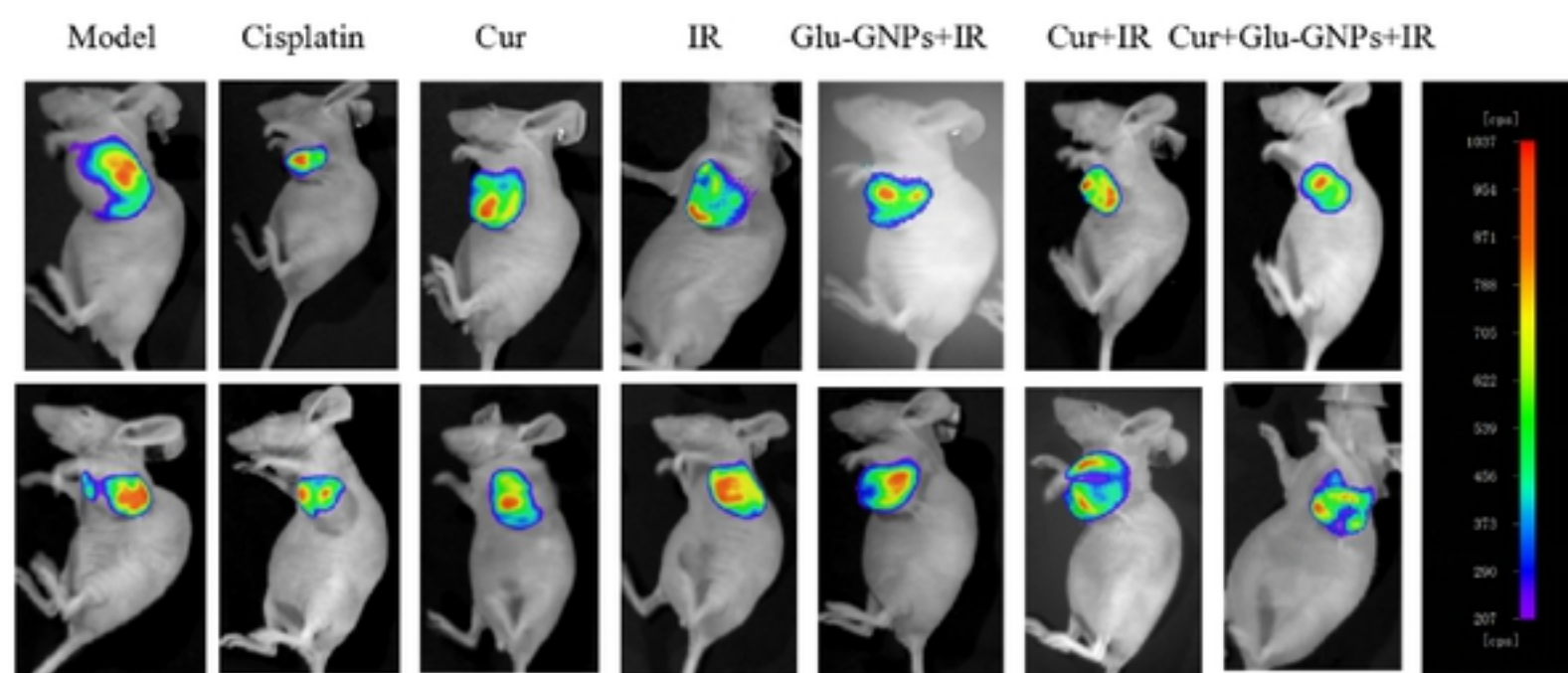
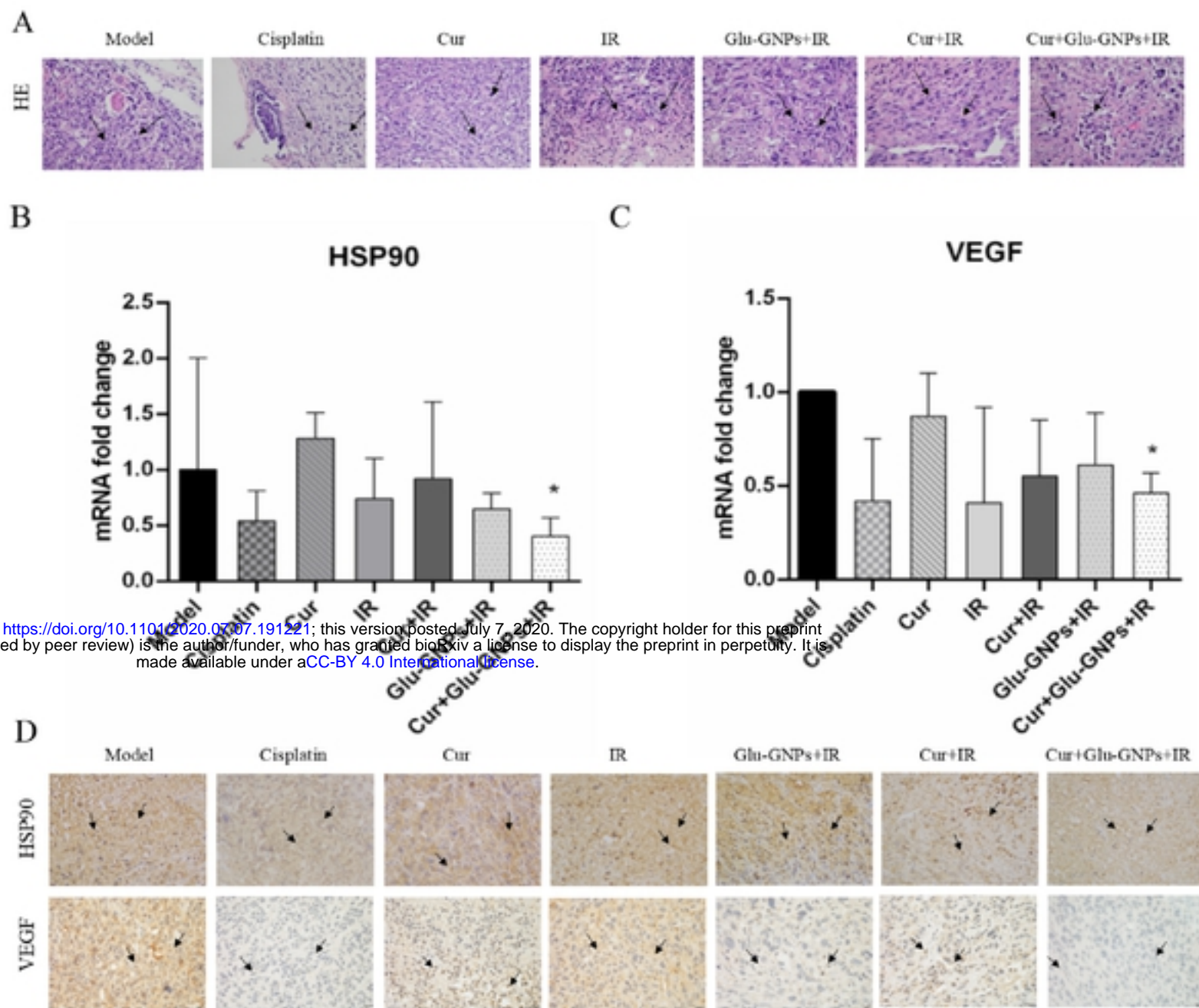


Fig 2



bioRxiv preprint doi: <https://doi.org/10.1101/2020.07.07.191221>; this version posted July 7, 2020. The copyright holder for this preprint (which was not certified by peer review) is the author/funder, who has granted bioRxiv a license to display the preprint in perpetuity. It is made available under aCC-BY 4.0 International license.



bioRxiv preprint doi: <https://doi.org/10.1101/2020.07.07.191221>; this version posted July 7, 2020. The copyright holder for this preprint (which was not certified by peer review) is the author/funder, who has granted bioRxiv a license to display the preprint in perpetuity. It is made available under aCC-BY 4.0 International license.